flow at velocity a bit less than the core value. The frequency of oscillations depends on flow speed, interelectrodes gap, and parameters of power supply. In the most cases, this value was $F = 10$–30 kHz under the experimental conditions. The regulation of power release was performed by means of electrical current change in a range $W_{\text{pl}} = 3$–17 kW. The maximal translational gas temperature in discharge zone was measured by optical spectroscopy at about $T_g \approx 3000$ K; therefore, the V-T relaxation length was expected to be around several centimeters [5]. Typical oscillograms are presented in Fig. 4*b*.

4 EXPERIMENTAL RESULTS

Figures 5*a* and 5*b* present typical experimental data obtained for the model configuration mentioned above. Figure 5*a* is the Schlieren image of undisturbed flow structure. Figure 5*b* shows the flow structure when the plasma generator was switched on. An extrusive layer excited by plasma and the first shock moved upstream are well seen. There are three important statements that might be considered due to analysis of the Schlieren images:

(1) the first shock shifts upstream;

(2) the angle of the first shock decreases comparing with initial situation and depends on plasma power; and

(3) the second shock loses its intensity.

The generation of new shock wave structure starts from the first discharge breakdown and is followed by a cylindrical unsteady shock wave (SW in the picture) and thermal cavern formation. The initial stage is shown on instant

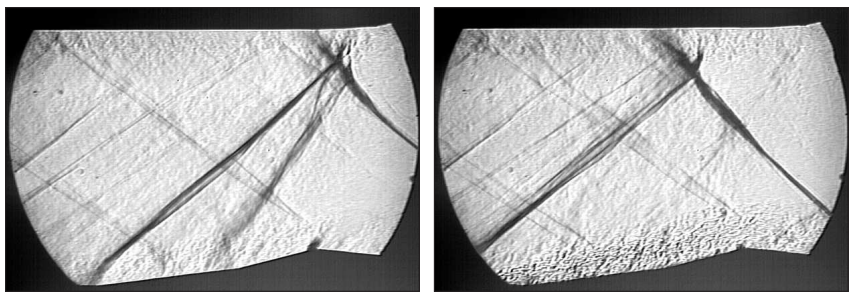

(*a*) (*b*)

Figure 5 Schlieren picture for undisturbed flow (*a*) and for plasma generation $W = 12$ kW (*b*)

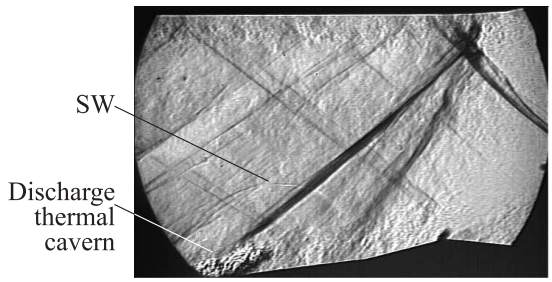

Figure 6 Schlieren image of initial stage of new shock structure formation. Delay 60 μs

Schlieren image in Fig. 6, which is recorded at 60 μs after the discharge initiation. Unfortunately, exact synchronization of Schlieren record and the discharge breakdown occurs rather difficult. To resolve the details of interaction at initial stage, an original Schlieren-streak technique was applied for visualization [9]. A main feature here is in application of the fast line-scan camera for Schlieren image acquisition along a predefined line of flowfield. In this particular case, the line of scanning was tuned in mid section of the channel $Y = 30$ mm.

Two extra problems were under experimental analysis based on processing of Schlieren-streak records:

(1) duration of transitional mode (time for the new configuration establishment); and

(2) stability of plasma-induced shock (remember that the discharge is principally unstable).

A new shocks pattern is established in approximately 0.2 ms that is well visible in Schlieren-streak image (Fig. 7). The first shock is stabilized in a new position; the second shock looks to be disappeared in short time. A bit more time is needed for a new reflected shock formation. The longest time elapses for the restoration of initial structure after the discharge was switched off. The period of the discharge oscillation is about 50 μs, which is 5 times longer than the temporal resolution of the visualization technique, but which is less than the shock structure renovation. Therefore, the Schlieren-streak images prove the statement on stability of new shocks position.

The decrease of shock angle indicates that the conditions for the model flown around are significantly modified, namely, the pressure losses can be expected less than under initial configuration. The pressure measurements prove this premise as shown in Figs. 8 and 9. The integration of the pressure distribution along the model gives the reduction of tangential force in factor 0.7. Figure 9 presents the data on the total pressure measurements (Pitot tube pressure) across the

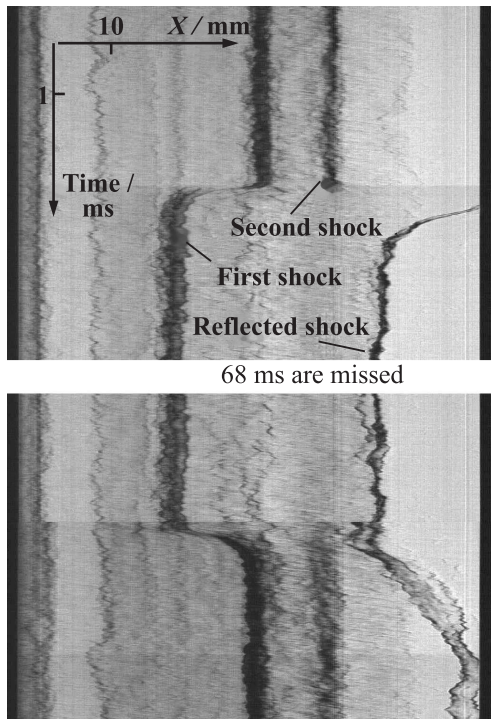

Figure 7 Schlieren-streak image, $Y = 29$ mm

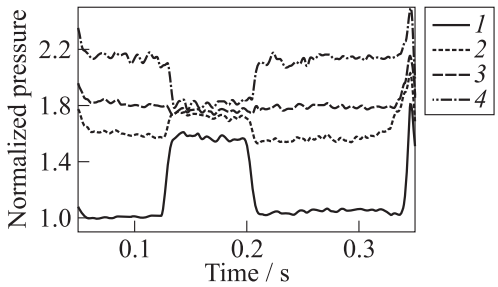

Figure 8 Static pressure redistribution on ramp under plasma generation, $W = 16.6$ kW: *1* — P_2/P_1; *2* — P_3/P_1; *3* — P_4/P_1; and *4* — P_5/P_1

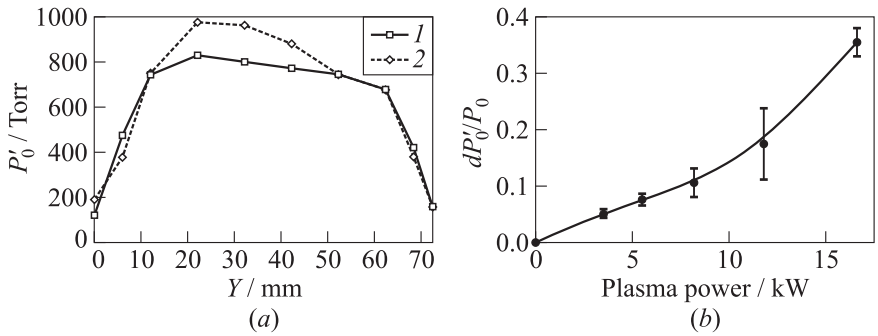

Figure 9 Plasma effect on total pressure downstream: (a) tranversal pressure distribution, $X = 210$ mm (*1* — no plasma and *2* — plasma on); and (b) total pressure vs. plasma power

channel downstream the model location. It can be considered the total pressure rise in the core of main flow, which reflects the reduction of the pressure losses in the model-associated shocks.

5 THE FIRST SHOCK ANGLE AND POSITION VERSUS PLASMA POWER

The Schlieren images allow recognizing the details of the flow structure (see Fig. 3). The first shock position X_3 was measured at $Y = 45$ mm (top wall has coordinate $Y = 60$ mm) due to irregular shock reflection on the wall. The shock's position X_1 corresponds with the point of regular reflection. It is calculated based on A1 and X_3. Figure 10 presents the graph of the first shock angle depending on the plasma power release at two values of initial Mach number. The calculated results for $M_0 = 2$ are shown here as well. Numerical modeling [8] of flow in experimental configuration was based on solution of three-dimensional (3D) time-dependent unstable Reynolds averaged Navier–Stocks equations (URANS-method). The behavior is unstable at low level of plasma power: dashed line connects the experimental point here. The accuracy of angle measurement is not worse than $\pm 0.5°$.

The graphs in Fig. 11 show the coordinates of shocks position at $Y = 45$ mm and on the top wall. The following statements can be written based on these results:

– zone of effective regulation of the shock position is covered by the power range $W_{pl} = 3$–15 kW. Following increase of the power can be useless. In dimensionless approach, it looks like follows:

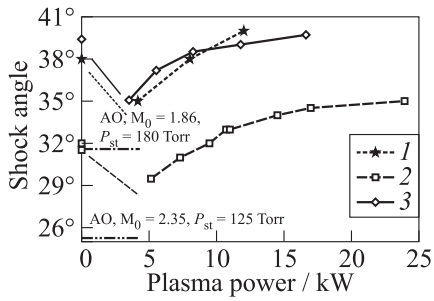

Figure 10 The first shock angle (*1* — $M_0 = 2$, and *2* — $M_0 = 2.35$) vs. plasma power (*3* — plasma on, $M_0 = 1.86$)

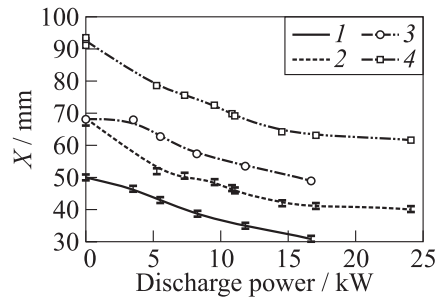

Figure 11 The first shock position at $Y = 45$ mm (*1* — $M_0 = 1.87$; and *2* — $M_0 = 2.35$); and on top wall (*3* — $M_0 = 1.87$; and *4* — $M_0 = 2.35$) vs. plasma power

$$w = \frac{W_{\rm pl}}{ZP_{\rm st}} = 2\text{–}10 \ \ [\text{kW}/(\text{bar} \cdot \text{cm})]$$

where w is the reduced plasma power; Z is the channel width;

– in this experimental series, the range of regulation only a bit higher than the wedge-electrodes distance $X = -18$ mm; and

– in this experimental approach, the shock at $M_0 = 2.35$ falls to the same position as for $M_0 = 1.87$ at plasma power $W_{\rm pl} = 10$–12 kW.

The data obtained show that the surface discharge burning upstream of the wedge leads to shifting of the root part of oblique shock upstream as well. At relatively small power release, the angle of the first shock is decreased significantly. The increase of the plasma power appeared in the rise of the first shock angle as it is presented in Fig. 10. The second shock occurs much weaker than under initial conditions. The power release below the value $W_{\rm pl} < 3$ kW causes an unstable behavior of the first shock. Such type of plasma-flow-model interaction can be called as "plasma screening" [6]. Downstream of this region, three main processes are in competition: cooling, turbulent mixing, and extra expansion due to energy relaxation from internal reservoir.

6 CONCLUDING REMARKS

The authors advocate a point of view that the plasma technology makes a sense for a correction of flow-field and support of high-speed flow regulation under the off-design operation modes. A theory [8] and the lab-scale experiments prove a

hope on effective, inertialess, and adjustable control of the flow structure and gas parameters. In the most cases, this method is much more effective than mechanical one. In some cases, there are no other methods to achieve a required result.

The transversal electrical discharge affects the flow similar to a soft wedge, whose angle depends on the electrical power release. At exceeding the value about $W/P_{\text{st}} \approx 10z$ W/Torr, where z is the discharge region depth, the flow separates [6] downstream with subsequent attachment or without it. The discharge generation is accompanied by the formation of the oblique shock. The amplitude, angle, and position of this shock wave can be regulated with the aid of electrical parameters variation. Specifically, the surface plasma generation near the inlet wedge is shown to regulate the angle of the first shock and to shift the shock wave in respect of the initial position.

In the case of air, a huge gradient postplasma extrusive layer is observed that is in accordance with an idea of the mechanism of slowed V-T relaxation. This layer "screens" the contoured model leading to some reduction of the pressure losses in the channel. The thickness and the length of this layer depend on static pressure of the gas and velocity of the flow. Despite of an unstable behavior of the discharge, the shocks' position was stable, predictable, and allowed regulation by means of discharge parameters. The experiments have demonstrated a promising ability of electrical discharge to improve the inlet's performance.

ACKNOWLEDGMENTS

Currently, this work is supported by MBDA-France. The authors appreciate Dr. A. Miller of MIPT for his help in numerical simulations.

REFERENCES

1. Merriman, S., E. Plonjes, and P. Palm. 2001. Shock wave control by nonequilibrium plasmas in cold supersonic gas flows. *AIAA J.* 39:1547–52.
2. Macheret, S., R. Miles, and M. Schneider. 2003. Comparative analysis of MHD and plasma methods of scramjet inlet control. AIAA Paper No. 2003-0170.
3. Bletzinger, P., B. N. Ganguly, D. VanWie, and A. Garscadden. 2005. Plasmas in high speed aerodynamics. Topical review. *J. Phys. D: Appl. Phys.* 38:R33–R57.
4. Shang, J. S., S. T. Surzhikov, R. Kimmel, *et al.* 2005. Mechanisms of plasma actuators for hypersonic flow control. *Progr. Aerospace Sci.* 41:642–68.
5. Leonov, S., V. Soloviev, and D. Yarantsev. 2006. High-speed inlet customization by surface electrical discharge. AIAA Paper No. 2006-0403.

6. Leonov, S., and D. Yarantsev. 2008. Near-surface electrical discharge in supersonic airflow: Properties and flow control. *J. Propul. Power* 24(6):1168–81.
7. Moreau, E., C. Louste, G. Artana, M. Forte, and G. Touchard. 2006. Contribution of plasma control technology for aerodynamic applications. *Plasma Proc. Polymers* 3:697–707.
8. Leonov, S. B., A. A. Firsov, D. A. Yarantsev, F. Falempin, amd A. Miller. 2009. Flow control in model supersonic inlet by electrical discharge. AIAA Paper No. 2009-7367.
9. Leonov, S. B. 2010. Visualization of unsteady electrical discharges in high-speed flow. Keynote lecture. *10th ASV Conference (International) Proceedings*. Nagar, Tamil Nadu, India. 1–11.